

Mechanical Response Characteristics Analysis of Tunnel Surrounding Rock during Near-Fault Construction

Tao Luo¹, Qingyun Huang¹, Yubo Chen^{2,*}, Jingmao Xu³ and Shuimei Chen¹

¹College of Resource Engineering, Longyan University, Longyan 364012, China

²International Joint Research Laboratory of Henan Province for Underground Space Development and Disaster Prevention, Henan Polytechnic University, Jiaozuo 454003, China

³Institute of National Defense Engineering, Academy of Military Sciences, Luoyang 471023, China

Received 1 October 2022; Accepted 29 December 2022

Abstract

The fault is often encountered in tunnel engineering. To reveal the mechanical response characteristics of the tunnel surrounding rock during construction near the fault, according to the actual trend of the fault and the different angles between the fault surface and the axis of the tunnel, the whole process of tunnel excavation was simulated by using MIDAS/GTS software. The deformation and failure characteristics of the surrounding rock in different sections were analyzed and the support strength was also analyzed. Results show that the bench excavation is better applied to the current geological characteristics, and the support strength can ensure the long-term stability of the surrounding rock of the tunnel. The construction excavation will cause some surface subsidence, but the subsidence is small. According to the design and a double-layer reinforcement network support strength, the excavation demand of the tunnel can be met. The qualitative and quantitative results are mutually verified and comprehensively judged to escort the construction process. The conclusions obtained in the study provide a significant reference to the tunnel construction near the fault.

Keywords: Tunnel engineering, Fault, Surrounding rock, Numerical simulation, Deformation

1. Introduction

The stability of tunnel surrounding rock is the key problem of tunnel engineering. Once the deformation or failure of surrounding rock appears, it will cause the tunnel collapse and bring huge loss to the construction. Soft structures such as faults and structural planes are the most common adverse geological phenomena in tunnel excavation. The section with faults is one of the most unstable sections of tunnel surrounding rock [1]. Most of the deformation and damage of tunnel surrounding rock are controlled by the structural plane of the fault. The distribution, characteristics and combination of the structures are the internal factors of the rock mass stability, which determines the stability of the rock mass, the boundary conditions, methods, scale and characteristics of the possible deformation and failure. Therefore, the study of deformation and failure of surrounding rock under the influence of faults is of great significance for tunnel excavation engineering.

In the excavation and construction of underground caverns, the fault is often encountered and must be dealt with effectively in the tunnel engineering. Many engineering practices and related studies have shown that the deformation and failure of tunnel surrounding rock is generally controlled by weak structural surfaces and faults. At the same time, the effect of fault on the deformation and failure of tunnel surrounding rock has been a fuzzy problem so far [2]. The study on the deformation and failure of tunnel surrounding rock has important theoretical significance and practical value, which provides certain convenience for tunnel excavation and construction and has certain practical

significance.

At present, there are many problems in engineering geomechanics caused by faults. The different types and changes of faults lead to the instability of the engineering rock mass [3]. However, the influence of the faults, especially the fragmentation faults on the deformation and failure of tunnel surrounding rock has not been well solved from the point of view of mechanics. Therefore, it is of great practical significance to analyze the stress, strain, deformation and damage of tunnel surrounding rock from the angle of engineering mechanics and geomechanics, so as to meet the needs of engineering practice.

2. State of the art

The destruction or excessive deformation of the surrounding rock, such as undue roof collapse, edge wall extrusion, floor uplift, floor water inrush, surrounding rock cracking, burst rock burst, and support fracture and so on, all of these are the characteristics of the instability of surrounding rock [4-10]. Because of the complexity and particularity of the surrounding rock geological conditions, many scholars have studied the stability of surrounding rock. So many methods of stability analysis of surrounding rock have been formed.

The numerical simulation method plays an important role in the study of surrounding rock stress and the development of deformation and destruction of surrounding rock, and then to quantitatively evaluate the stability of surrounding rock. Because this method can not only solve the problem of the stress analysis of various non-homogeneous, nonlinear, weak structural planes, and the

*E-mail address: 569079218@qq.com

ISSN: 1791-2377 © 2023 School of Science, IHU. All rights reserved.

doi:10.25103/jestr.161.19

rheological properties, but also can simulate the effectiveness of various supporting schemes and the influence of different construction procedures on the stability of the surrounding rock. Wang et al. studied large deformation mechanics mechanism and rigid-gap-flexible-layer supporting technology of soft rock tunnel, and they analyzed the thermal radiation characteristics of stress evolution of a circular tunnel excavation under different confining pressures [11]. Luo et al. analyzed the parameters deterioration rules of surrounding rock for deep tunnel excavation based on unloading effect [12]. Wang et al. conducted the analysis of damage evolution characteristics of surrounding rock in deep anchorage cavern under dynamic loading [13]. Wang et al. studied the microseismic distribution characteristics near-fault mining induced and its influencing factors [14]. Yoo & Cui studied the effect of new tunnel construction on structural performance of existing tunnel lining [15]. Aygar conducted the evaluation of new Austrian tunnelling method applied to Bolu tunnel's weak rocks [16]. Aygar & Gokceoglu analyzed the problems encountered during a railway tunnel excavation in squeezing and swelling materials and the engineering measures [17]. Tyagi & Lee studied the influence of tunnel failure on the existing tunnel in improved soil surround [18].

Many scholars have done a lot of work about anchor cable, bolt force and concrete support during tunnel excavation. Wu et al. analyzed damage characteristics and constitutive model of lightweight shale ceramsite concrete under static-dynamic loading [19]. Wang et al. analyzed the coupling effect of tension and reverse torque of anchor cable under different conditions [20]. Nguyen et al. studied the influence of tunnel shape on tunnel lining behaviour [21]. Yokota et al. developed a new deformation-controlled rock bolt by using numerical modelling and laboratory verification [22]. Ranjbaria et al. proposed the practical method for the design of pretensioned fully grouted rockbolts in tunnels [23]. Shimamoto & Yashiro proposed new rockbolting methods for reinforcing tunnels against deformation [24].

The rest of the study is organized as follows. Section 3 gives the relevant engineering background, the computational model and calculation scheme. Section 4 presents the results analysis and discussion, and finally, the conclusions are summarized in Section 5.

3. Methodology

3.1 Engineering background

The right tunnel is 1011 m long and the left tunnel is 1016 m long, with a separated double tunnel arrangement, the entrance of the right tunnel is on a flat curve of radius 1300 mm and the exit is on a straight line. The entrance of the left tunnel is on a flat curve of radius 1550 mm and the exit is on a straight line. The main tunnel has a clear width of 14 m and a clear height of 5 m, with a traffic lane of 3.75 m × 2 m, a lateral width of 0.5 m + 0.75 m and a maintenance lane of 0.75 m + 0.75 m. The tunnel envelope is classified as class IV 439.3 m and class V 1587.6 m. The engineering geology and borehole exposures show that the tunnel is an outcrop of Jurassic rhyolite and tuffaceous rhyolite, with six major faults passing through it. A representative F1 fault was selected for the tunnel construction simulation, and its engineering geological conditions are as follows: there is an obvious fault surface at around YK145 + 577 m, intersecting the route obliquely. The rock body is strongly weathered and

broken at this place, which affects the stable of the tunnel surrounding rock.

3.2 Computational model

The elastic-plastic model of GTS simulates the elastic-fully plastic intrinsic relationship, and its typical stress-strain curve is shown in Fig. 1. The stress is proportional to the strain until it reaches the yield point, and the stress-strain relationship is horizontal when it exceeds the yield point [25].

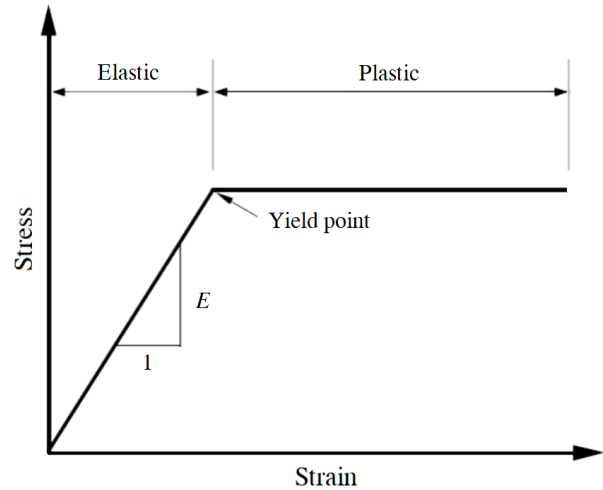


Fig. 1. Elastic-plasticity relationship.

The elastoplastic material models in MIDAS/GTS are Mohr-Coulomb, Tresca, Von Mises, Drucker-Prager, Hoek-Brown, Drucker-Prager and Hoek-Brown model. For the structural characteristics of the tunnel and the fault, a typical section is selected and the Mohr-Coulomb criterion is used for the 3D finite element calculation. The yield function is as follows:

$$F(\underline{\sigma}) = \frac{\sin\phi}{3} I_1 + \sqrt{J_2} \left(\cos\theta - \frac{1}{\sqrt{3}} \sin\theta \sin\phi \right) - c \cos\phi = 0 \quad (1)$$

$$I_1 = \sigma_x + \sigma_y + \sigma_z \quad (2)$$

$$J_2 = \frac{1}{6} [(\sigma_x - \sigma_y)^2 + (\sigma_y - \sigma_z)^2 + (\sigma_z - \sigma_x)^2] + \tau_{xy}^2 + \tau_{yz}^2 + \tau_{zx}^2 \quad (3)$$

$$J_3 = s_x s_y s_z + 2\tau_{xy} \tau_{yz} \tau_{zx} - s_x \tau_{yz}^2 - s_y \tau_{zx}^2 - s_z \tau_{xy}^2 \quad (4)$$

$$\theta = \frac{1}{3} \cos^{-1} \left(\frac{3\sqrt{3} J_3}{2 J_2^{3/2}} \right) \quad (5)$$

where, ϕ is internal friction angle.

The support parameters were selected for simulation by engineering analogy method and combined with the convergence measurement around the hole in the later construction. After obtaining complete and reliable data of more than one section, the original estimated parameter values were revised twice, and finally the analysis results were close to the actual ones.

Based on the elasto-plastic theory and engineering analogy, the range of the model was usually selected according to the span and height of the tunnel: the outer boundary was taken as 3-5 times of the span, and the upper

and lower boundaries were taken as 3-5 times of the height, outside the range could be considered as not affected by excavation and other construction factors, i.e. the stress and displacement caused by excavation and other construction could be ignored at these boundaries. At the same time, the model was guaranteed to be free of rigid body displacements and rotations.

To make the simulation results effectively close to the engineering reality and to truly reveal the fault direction and level of production on the construction excavation, according to the established route of the tunnel, the model numerical analysis was set to F1 fault tunnel. The left and right sides were taken as 4 times the diameter of the tunnel 45 m, 4 times the height of the tunnel 30 m in the vertical direction downward and upward to the surface, and the length of the longitudinal tunnel excavation was 40 m for simulation. The initial stress field of the rock was considered only for self-weight stress, and the effect of tectonic stresses was not considered. The model was divided by tetrahedral mesh cells, and the number of nodes in the numerical model was 12619 and the number of cells is 44211, as shown in Figs. 2. and 3.

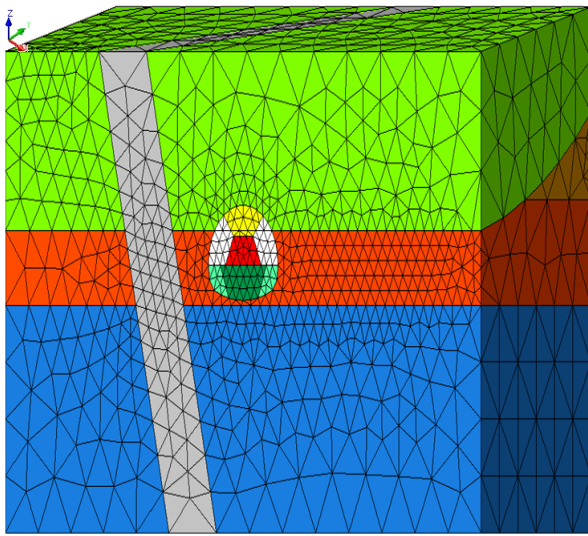


Fig. 2. The computational model with F1 fault.

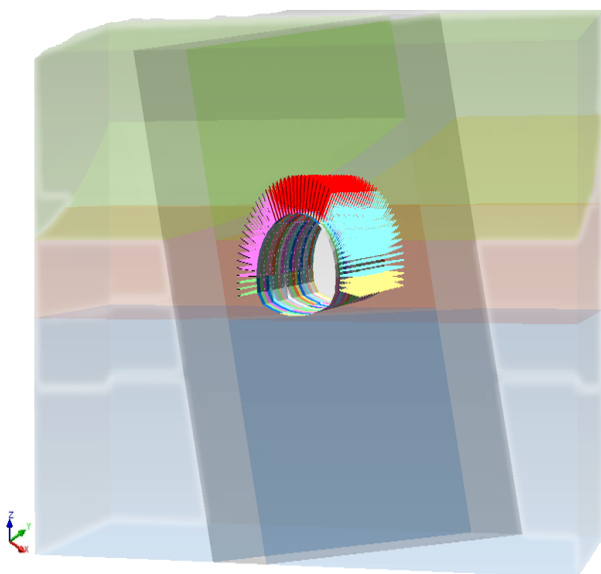


Fig. 3. The lining support of the tunnel.

The physical and mechanical parameters of the surrounding rock at all levels of the model and the tunnel

support parameters are shown in Tables 1 and 2. The steel arches in the initial shotcrete support were converted to the concrete according to the mechanical index to simplify the calculation.

Table 1. Physical and mechanical parameters of the model.

Name	Elastic modulus (GPa)	Poisson's ratio	Internal friction angle (°)	Cohesion (MPa)	Density (kN/m ³)
Gravel layer	0.8	0.40	20	0.08	19
Tuff	0.9	0.40	23	0.1	22.5
Strongly weathered tuff	0.8	0.40	20	0.08	21
Slightly weathered rhyolite	1.5	0.35	30	0.4	22
Unweathered rhyolite	2	0.33	33	0.5	23.7
Rhyolite	2.5	0.32	35	0.6	24
Fractures	0.5	0.45	10	0.016	16

Table 2. Parameters of tunnel support.

Name	Elastic modulus (GPa)	Poisson's ratio	Size (mm)	Material
Concrete initial support	28	0.2	280	C25
Anchor rods hollow grouting	160	0.3	Diamere 25	Steel

3.3 Calculation scheme

To effectively reflect the deformation, stress and other states of the tunnel envelope at each stage of the construction excavation process, the simulation calculations were performed on the tunnel model with F1 fault based on the existing design excavation and support methods to analyze the stress and strain distribution and change patterns. The processing function of program unit (activation & passivation) and the concept of equivalent release load of tunnel excavation were used to simulate the whole process of tunnel construction, and the construction methods and processes were strictly in accordance with the site.

4. Results analysis and discussion

4.1 Analysis of stress field of surrounding rock

In the process of construction simulation, the longitudinal excavation (X - direction) mainly studies the geological condition of the tunnel excavation face, and the possible damage form and the mechanical dynamics of the surrounding rock are preliminarily determined. The stress changes in surrounding rocks are mainly observed in horizontal stress (Y - direction) and vertical stress (Z -direction). After the excavation of the tunnel, the surrounding rock is in the initial stress state; after the excavation of the stress redistribution and the release of the residual stress in the local crust, the displacement of the surrounding rock formation is relaxed and the new temporary equilibrium state is called the two stress state, and the stress state around the tunnel after the support is called the three stress state. The load release coefficient is usually used to simulate the mechanical process. The load release process is as follows: 40% load is released from the surrounding rock at the current excavation stage, and 30% load is released in two subsequent construction sections. Figs. 4 and 5 are the horizontal stress distribution of the whole surrounding rock of typical construction sections.

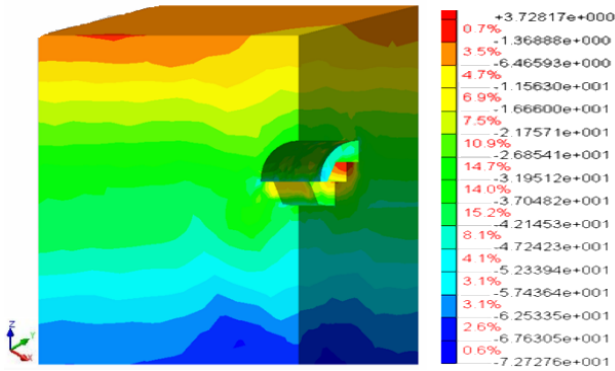


Fig. 4. The horizontal stress distribution S_{yy} of tunnel surrounding rock at the excavation adjacent to the fault.

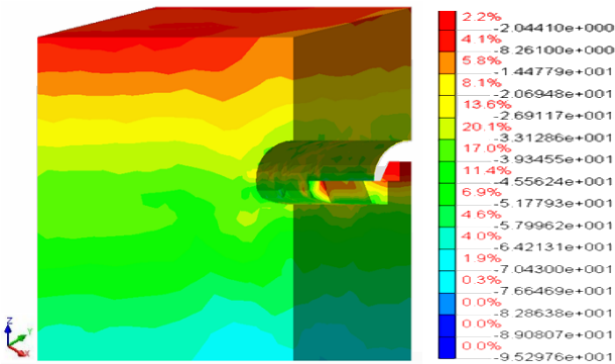


Fig. 5. The horizontal stress distribution S_{yy} of tunnel surrounding rock after excavation through the fault.

As seen from Figs. 4 and 5, from the initial progress of tunnel excavation to the vicinity of the fault, then through the fault until tunnel penetration, there is no extensive tensile stress area in the surrounding rock, and the local tensile stress concentration area is affected by the step-by-step method of excavation and distributed around the retained core soil, which has little influence. For the overlying area of this tunnel site is close to the tunnel entrance, the overlying soil thickness is shallow and loose, the influence of the fault is not very obvious in terms of stress, which will be analyzed in combination with the later displacement and settlement.

As seen from Figs. 6 and 7, the overall development trend is similar to the horizontal stress. The concentration of compressive stress at the foot of the arch on both sides of the surrounding rock is also more obvious, which belongs to the key observation range of the later monitoring.

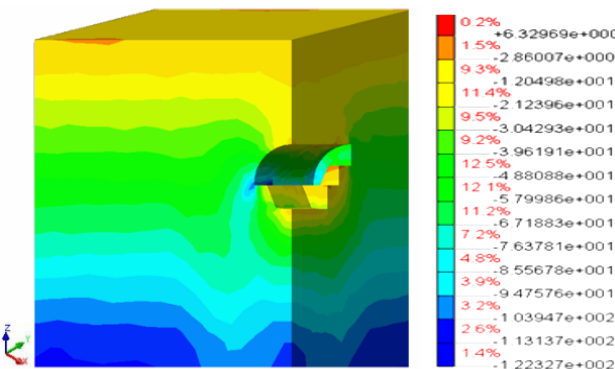


Fig. 6. The vertical stress distribution S_{zz} of tunnel surrounding rock at the excavation adjacent to the fault.

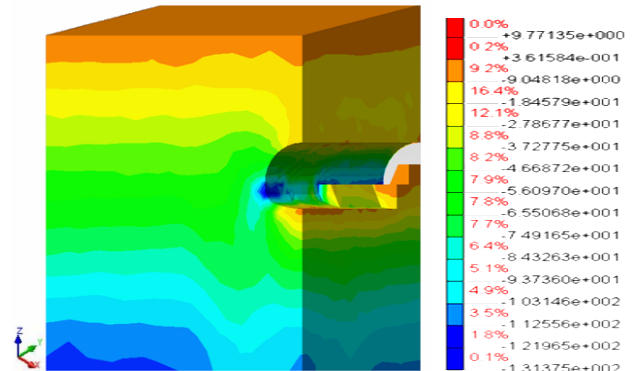


Fig. 7. The vertical stress distribution S_{zz} of tunnel surrounding rock after excavation through the fault.

4.2 Analysis of displacement field of surrounding rock

To effectively illustrate the impact of tunnel excavation on the surrounding rock and the mechanism of action, reveal the displacement concentration area, and provide scientific reference data for the prevention of local collapse and construction of similar projects, it is proposed to select DY, DZ displacement and other linear diagrams to assist in illustration, and combine with the actual measurement data on site to improve the analysis of each result.

Vault subsidence DZ and peripheral convergence displacement value DY is a comprehensive reflection of the surrounding rock, surrounding rock conditions and support effect during tunnel excavation, which is an important mandatory measurement item as the whole process of construction. The measurement results of this study can be used to judge the stability of the surrounding rock, the appropriateness of the initial support and the filling time of the lining and the back arch. Figs. 8 and 9 show the convergence value of displacement in the direction of DY in the typical construction section, and Figs. 10 and 11 show the convergence value of displacement in the direction of DZ in the typical construction section.

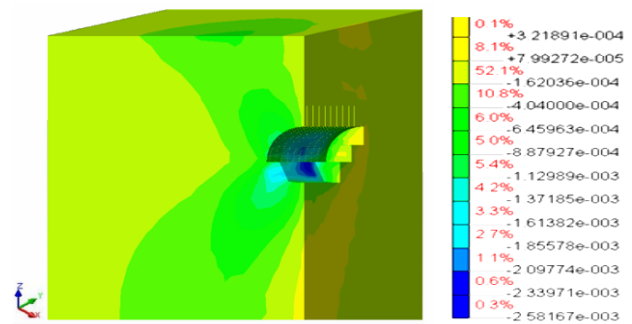


Fig. 8. DY direction convergent displacement of tunnel surrounding rock at the excavation adjacent to the fault.

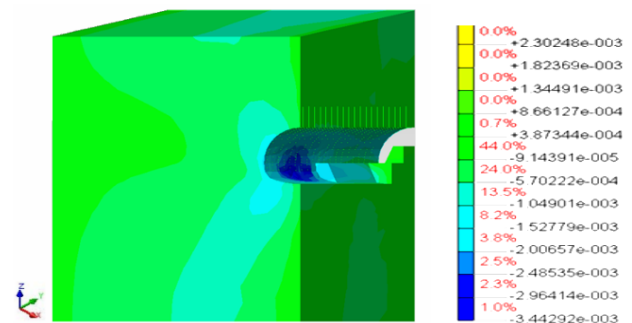


Fig. 9. DY direction convergent displacement of tunnel surrounding rock after excavation through the fault.

When the tunnel excavation is close to the fault zone, the surrounding rock is affected by the fault zone, displacement began to gradually rise, the displacement of the unexcavated lower step area is larger. By the fault trend and dip angle mechanism of action, the calculation of comparison can be obviously found that with the excavation development, the displacement concentration area closely follows the fault trend and tends to step change, the impact is significant. The right side of the surrounding rock affected by the range is significantly larger than the left.

Influenced by the fault, when two kinds of rocks with different mechanical properties come into contact, the displacement of the corresponding excavation construction section rises significantly, and finally the peripheral convergence of the surrounding rock on the left side is 3.5 mm, and on the right side is about 4.0 mm, there is a certain bias pressure effect.

DZ displacement is mainly to study the influence of tunnel excavation on the surrounding rock vault and elevation arch and the mechanism of action, revealing the displacement concentration area, providing scientific reference data for the prevention of local collapse and later construction. Compared with DY, the data of vault subsidence change in the direction of DZ is more obvious, which can clearly show the surrounding rock under the influence of fault easy to destroy area.

With the passage of the fault excavation, it is obvious that under the influence of the fault, the maximum settlement of the top of the surrounding rock arch increases from 1.19 mm to 3.91 mm and 5.31 mm at the beginning of excavation, and finally 5.35 mm is stable, while the elevation of the supine arch converges from 1.83 mm to 6.11 mm to 6.73 mm to the final 6.93 mm, which shows that the supine arch section up-drum situation is serious, and the local area exceeds the settlement of the arch, it is recommended to close early and replace the fill in time.

4.3 Analysis of shotcrete force

The excavation of the tunnel is inevitably accompanied by the redistribution of the stress and the development of the radial displacement of the tunnel. In general, the support form of sprayed concrete plus anchor rods is used to improve the bearing conditions of the surrounding rock, so as to improve the bearing capacity of the surrounding rock accordingly.

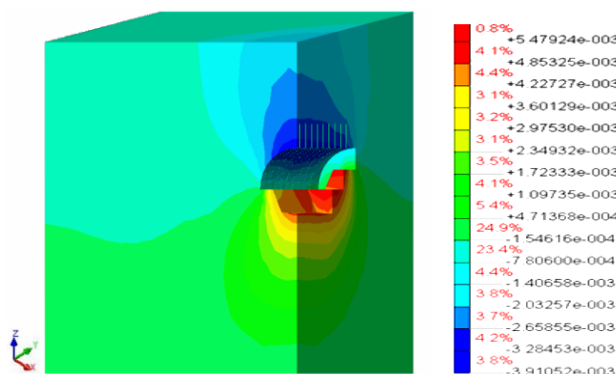


Fig. 10. DZ direction convergent displacement of tunnel surrounding rock at the excavation adjacent to the fault.

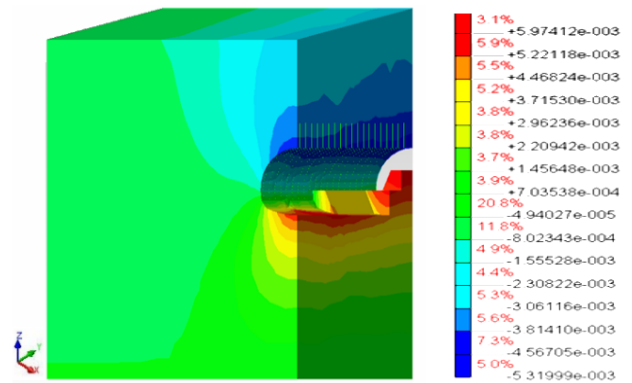


Fig. 11. DZ direction convergent displacement of tunnel surrounding rock after excavation through the fault.

From the current design of the support structure, the sprayed concrete is the only means of support that can firmly adhere to the wall of the surrounding rock over a large area, and is also an effective mean of support applicable to all kinds of surrounding rock, its role is mainly through the bonding of sprayed concrete and the wall to transfer the axial force to the surrounding rock, in the direct prevention of increased relaxation of the surrounding rock and unstable rock falling at the same time, giving the internal pressure of the surrounding rock, so that the surrounding rock becomes one.

In the MIDAS/GTS program, the plane strain plate units are used to simulate the support effect of shotcrete. It is specified that the plane strain unit has no strain term in the thickness direction, and the unit degrees of freedom are only two translational degrees of freedom in the X- and Y- directions, and the stress symbols and directions are the same as those of the solid unit surrounding rock, both with reference to the overall coordinate system and following the right-hand rule. Figs. 12 and 13 show the maximum principal stress of the initial sprayed concrete in the surrounding rock.

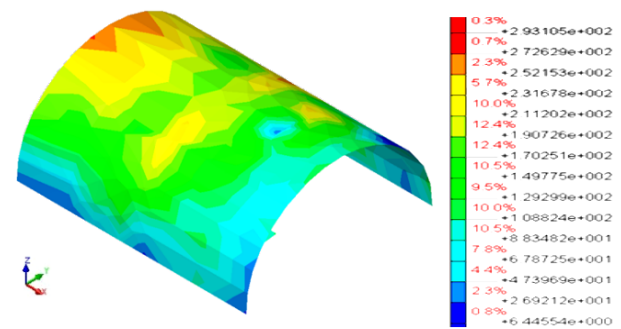


Fig. 12. Maximum principal stress of initial shotcrete in the surrounding rock at the excavation adjacent to the fault.

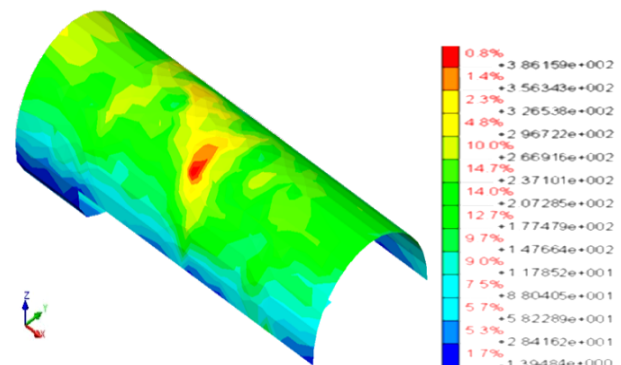


Fig. 13. Maximum principal stress of the initial sprayed concrete in the surrounding rock after excavation through the fault.

As seen from Figs. 12 and 13, the simulation analysis of the general tensile stress of the sprayed layer basically meets its strength requirements, but the maximum tensile stress at local locations exceeds its allowable tensile strength.

The damage of shotcrete is mainly shear damage and tensile damage, controlled by tensile and shear stresses, which can be clearly found from Figs. 12 and 13, the force of shotcrete at the fault is obviously different from that of the sprayed layer in the general surrounding rock area, with a final tensile stress of 4.38 MPa, which can be improved by using local strengthening measures.

4.4 Analysis of anchor rod force

Anchor rod is one of the important support means to maintain the stability of surrounding rock and ensure construction safety during the tunnel construction, and it is also the only support method to reinforce surrounding rock from inside. It can improve the shear strength of the fractured surrounding rock, also can improve the physical index of the surrounding rock, moreover, which can link some discontinuous rock blocks together, and basically does not occupy the operation space, and has good constructability. After the construction is completed, it can also function as part of the permanent support structure to a certain extent, so it is widely used.

Anchor rod is a type of point support. To give full play to the effect of anchor rod, it is necessary to play the role of group anchor, i.e. to solve the relationship between the surrounding rock conditions and the length and interval of anchor rod. According to the actual construction on site, the simulated length of anchor rod using line unit is 4 m. The stress distribution of anchor rod is shown in Figs. 14 and 15.

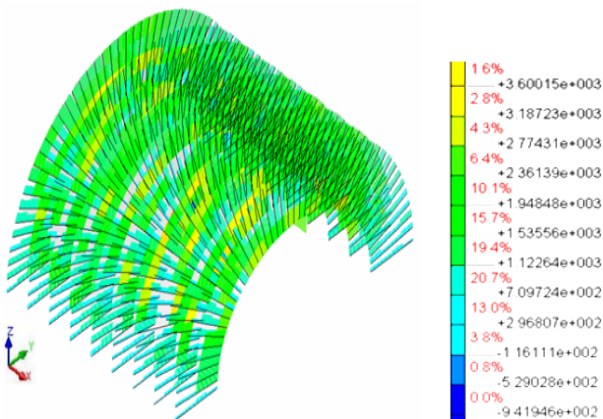


Fig. 14. Anchor stress distribution at the excavation adjacent to the fault.

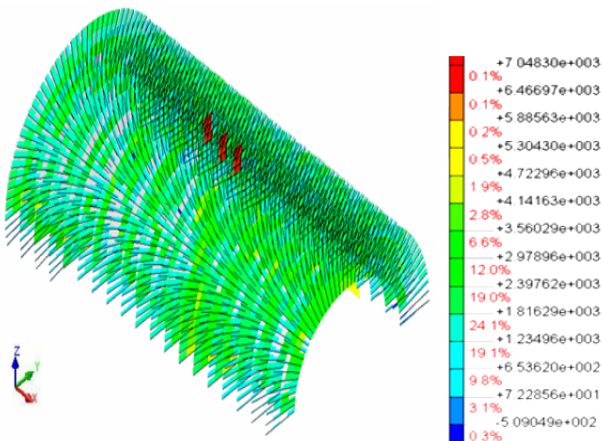


Fig. 15. Stress distribution of anchors after excavation through faults.

As seen from Figs. 14 and 15, the stress state of the group anchors in different construction sections of the surrounding rock. The anchor stresses are basically symmetrically distributed, with the greatest force at the vault anchors, mainly concentrated in the range of 1-2 m from the tunnel excavation profile, with a size of 38 MPa, i.e. the greatest force in the central region, and gradually decreasing to both sides of the tunnel.

With the continuous excavation of the tunnel, the stress on the reinforcement anchor rod increases significantly when approaching the fault zone, with a value of 76 MPa, while the stress distribution on the anchor rod in the rest of the buried section of the surrounding rock is relatively average, with no abnormal changes. After the tunnel construction being completed, the largest anchor stress area was concentrated in the lower part of the surrounding rock sidewall, with a maximum value of 89 MPa, which coincided with the displacement and stress concentration area in the previous section and was the key area for monitoring.

5. Conclusions

In this study, the geotechnical and tunnel analysis system MIDAS/GTS was used to establish the elastoplastic numerical model of typical faults and the specific construction section was selected to comprehensively analyze the stability of the surrounding rock under the influence of adjacent faults. The main conclusions are obtained as following:

(1) From the feedback results of the numerical simulation, the step-by-step excavation method is better applied to the current geological properties, and the support strength can ensure the long-term stability of the surrounding rock. It is recommended to carry out regular monitoring and measurement according to the actual construction conditions, and to increase the monitoring frequency for the local dangerous areas.

(2) The 1-2 additional displacement monitoring sections should be appropriately set in the area the fault located, and the frequency of field measurement should be increased to provide quantitative theoretical data to grasp the scope of the fault affected area. The observation and recording of geological statements can well define the nature of the surrounding rock. The qualitative and quantitative results are verified with each other and comprehensive judgments are made to escort the construction process.

(3) Since the F1 fault located in the tunnel is shallow, the construction excavation will cause part of the surface settlement, but the value is small, the support strength can meet the excavation needs. The simulation only considered the case of the spray layer support alone, so the surrounding rock stress exceeds the allowable stress of the spray layer. In the actual construction, the double-layer reinforcement network should be used in the spray layer, which can effectively improve the strength of the spray layer meeting the safety requirements of the support body.

For a long time, there has been a lack of a reasonable evaluation index for tunnel stability evaluation. For tunnel engineering, no matter what type of caverns is, the surrounding rock often does not reach the state of destruction when the equivalent plastic strain passes through the whole section. Only when the plastic strain develops to a certain degree in the plastic zone of the surrounding rock,

the potential failure surface is formed in the surrounding rock to reach the state of failure. In view of the special geological existence of the fault, the possible plastic strain range of the tunnel surrounding rock is preliminarily grasped, which will be of the reference for the tunnel construction.

Acknowledgements

The authors are grateful for the support provided by Fujian Provincial Education Hall Youth Fund, China (JAT160494).

This is an Open Access article distributed under the terms of the Creative Commons Attribution License.



References

1. Xu, Q. W., Cheng, P. P., Zhu, H. H., Ding, W. Q., Li, Y. H., Wang, W. T., Luo, Y., "Progressive damage model test and numerical simulation of cross-fault tunnel surround rock". *Journal of Rock Mechanics and Engineering*, 35(3), 2016, pp. 433-445.
2. Zeng, M., Yu, D. X., Xue, G. C., Li, P., Fan, L., Peng, S. Q., Qi, B. X., "Numerical simulation study on the mechanical response of tunnel under the action of vertical fault misalignment". *Journal of Wuhan University of Technology*, 42(8), 2020, pp. 63-68.
3. Gong, Q. M., Wang, Y., Lu, J. W., Wu, F., Xu, H. Y., Ban, C., "Preliminary classification of fault zones based on the impact on TBM tunnel construction". *Journal of Railway*, 43(9), 2021, pp. 153-159.
4. Qi, B. X., Wang, F., Chen, J. L., "Numerical simulation of structural response of tunnels crossing faults under the misalignment of viscous slip faults". *Building Structures*, 50(S2), 2020, pp. 753-758.
5. Lee, W. F., Ishihara, K., "Forensic diagnosis of a shield tunnel failure". *Engineering Structures*, 32(7), 2010, pp. 1830-1837.
6. Kontogianni, V., Papantonopoulos, C., Stiros, S., "Delayed failure at the Messochora tunnel, Greece". *Tunnelling and Underground Space Technology*, 23(3), 2008, pp. 232-240.
7. Fraldi, M., Guarracino, F., "Limit analysis of progressive tunnel failure of tunnels in Hoek-Brown rock masses". *International Journal of Rock Mechanics and Mining Sciences*, 50, 2012, pp.170-173.
8. Oliveir, D., Diederichs, M. S., "Tunnel support for stress induced failures in Hawkesbury Sandstone". *Tunnelling and Underground Space Technology*, 64, 2017, pp. 10-23.
9. Hsu, S. C., Chiang, S. S., Lai, J. R., "Failure mechanisms of tunnels in weak rock with interbedded structures". *International Journal of Rock Mechanics and Mining Sciences*, 41(3), 2004, pp. 489-489.
10. Koneshwaran, S., Thambiratnam, D. P., Gallage, C., "Blast response and failure analysis of a segmented buried tunnel". *Structural Engineering International*, 25(4), 2015, pp. 419-431.
11. Wang, S. R., Liu, Z. W., Qu, X. H., Fang, J. B., "Large deformation mechanics mechanism and rigid-gap-flexible-layer supporting technology of soft rock tunnel". *China Journal of Highway and Transport*, 22(6), 2009, pp. 90-95.
12. Luo, T., Wang, S. R., Zhang, C. G., Liu, X. L., "Parameters deterioration rules of surrounding rock for deep tunnel excavation based on unloading effect". *DYNA*, 92(6), 2017, pp. 648-654.
13. Wang, G. Y., Wang, T. T., Wang, S. R., He, Y. S., Kong, F. L., Fan, J. Q., "Analysis of damage evolution characteristics of surrounding rock in deep anchorage cavern under dynamic loading". *Journal of Engineering Science and Technology Review*, 13(3), 2020, pp. 96-105.
14. Wang, S. R., He, S. N., Li, C. Y., Yan, W. F., Zou, Z. S., "Near-fault mining induced microseismic distribution characteristics and its influencing factors". *Tehnicki Vjesnik-Technical Gazette*, 24(2), 2017, pp. 535-542.
15. Yoo, C., Cui, S. S., "Effect of new tunnel construction on structural performance of existing tunnel lining". *Geomechanics and Engineering*, 22(6), 2020, 497-507.
16. Aygar, E. B. "Evaluation of new Austrian tunnelling method applied to Bolu tunnel's weak rocks". *Journal of Rock Mechanics and Geotechnical Engineering*, 12(3), 2020, 541-556.
17. Aygar, E. B., Gokceoglu, C., "Problems encountered during a railway tunnel excavation in squeezing and swelling materials and possible engineering measures: a case study from Turkey". *Sustainability*, 12(3), 2020, pp. 1166.
18. Tyagi, A., Lee, F. H., "Influence of tunnel failure on the existing large-diameter tunnel in improved soil surround". *Tunnelling and Underground Space Technology*, 120, 2022, pp. 104276.
19. Wu, X. G., Wang, S. R., Yang, J. H., Zhao, J. Q., Chang, X., "Damage characteristics and constitutive model of lightweight shale ceramics concrete under static-dynamic loading". *Engineering Fracture Mechanics*, 259, 2022, pp. 108137.
20. Wang, S. R., Wang, Z. L., Chen, Y. B., Wang, Y. H., Huang, Q. X., "Mechanical performances analysis of tension-torsion coupling anchor cable". *International Journal of Simulation Modelling*, 19(2), 2020, pp. 231-242.
21. Nguyen, T. T., Do, N. A., Karasev, M. A., Kien, D. V., Dias, D., "Influence of tunnel shape on tunnel lining behaviour". *Proceedings of the Institution of Civil Engineers-geotechnical Engineering*, 174(4), 2021, pp. 355-371.
22. Yokota, Y., Zhao, Z. Y., Nie, W., Date, K., Iwano, K., Koizumi, Y., Okada, Y., "Development of a new deformation-controlled rock bolt: Numerical modelling and laboratory verification". *Tunnelling and Underground Space Technology*, 98, 2020, pp. 103305.
23. Ranjbaria, M., Fahimifar, A., Oreste, P., "Practical method for the design of pretensioned fully grouted rockbolts in tunnels". *International Journal of Geomechanics*, 16(1), 2016, pp. 04015012.
24. Shimamoto, K., Yashiro, K., "New rockbolting methods for reinforcing tunnels against deformation". *International Journal of Rock Mechanics and Mining Sciences*, 147, 2021, pp. 104898.
25. Barchukova, T. N., Zavrak, N. V., "Calculation of short length pile with widening using modern computers". *Technical Journal*, 9(2), 2015, pp. 177-179.